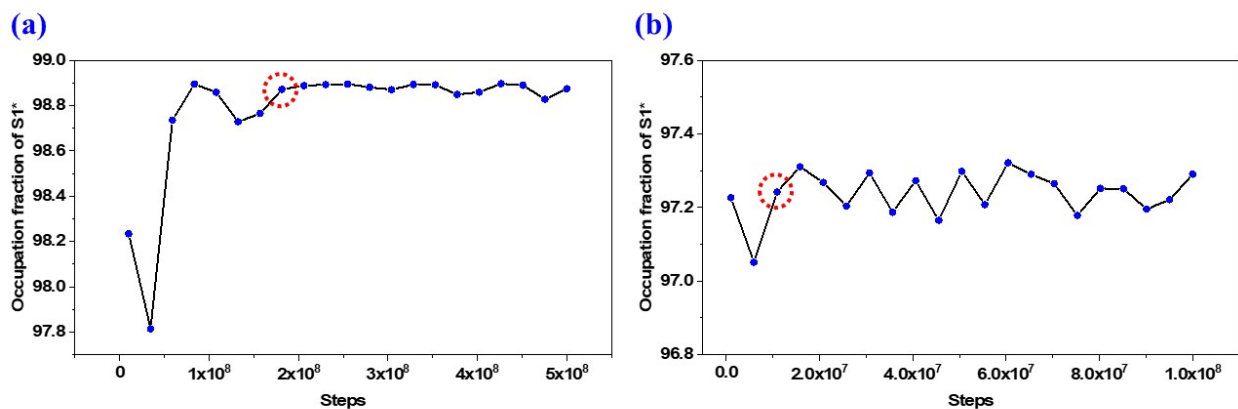Supporting Information

Migration of Zeolite-Encapsulated Pt and Au under Reducing Environments

Dianwei Hou[a], Christopher J. Heard[a]*

[a]Department of Physical and Macromolecular Chemistry, Faculty of Science, Charles University in Prague, 128 43 Prague 2, Czech Republic. *heardc@natur.cuni.cz

# 1.	Kinetic Monte Carlo simulation of Pt@LTA

(a)

(b)

Figure S1 Occupation percentage of the global minimum site (S1*) from kinetic Monte Carlo simulations of Pt@LTA at 800 (a) and 1000 K (b) with various simulation durations. Red circles mark the number of steps required to reach equilibration, from which the equilibration time for the system is calculated – defined as the length of time required to reach a converged occupation percentage.

2. Ab Initio Molecular Dynamics (AIMD)
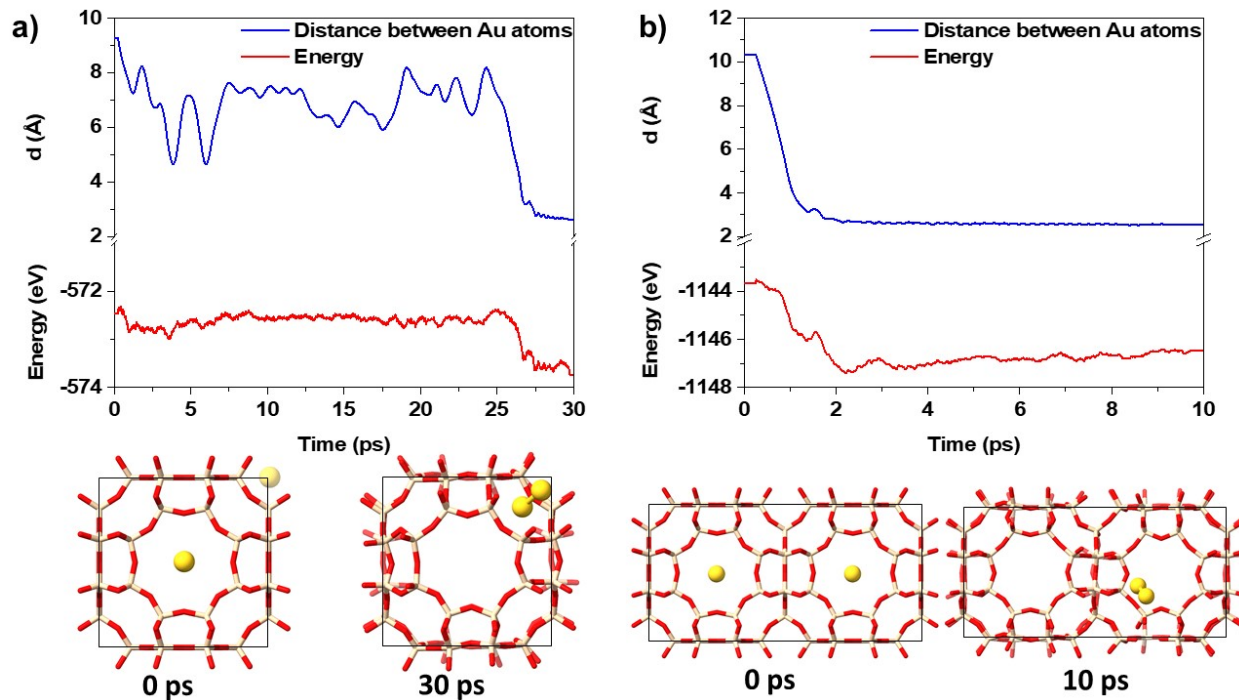
Figure S2 Ab Initio molecular dynamics simulations within the NVT ensemble were run at an elevated temperature of 450 K, with a timestep of 0.5 fs for two initial configurations, a) Au atoms located in adjacent α and β-cages. b) Au atoms located in adjacent α-cages.

3.   Kinetic Monte Carlo simulation of PtCO@LTA

(a)

(b)

(c)
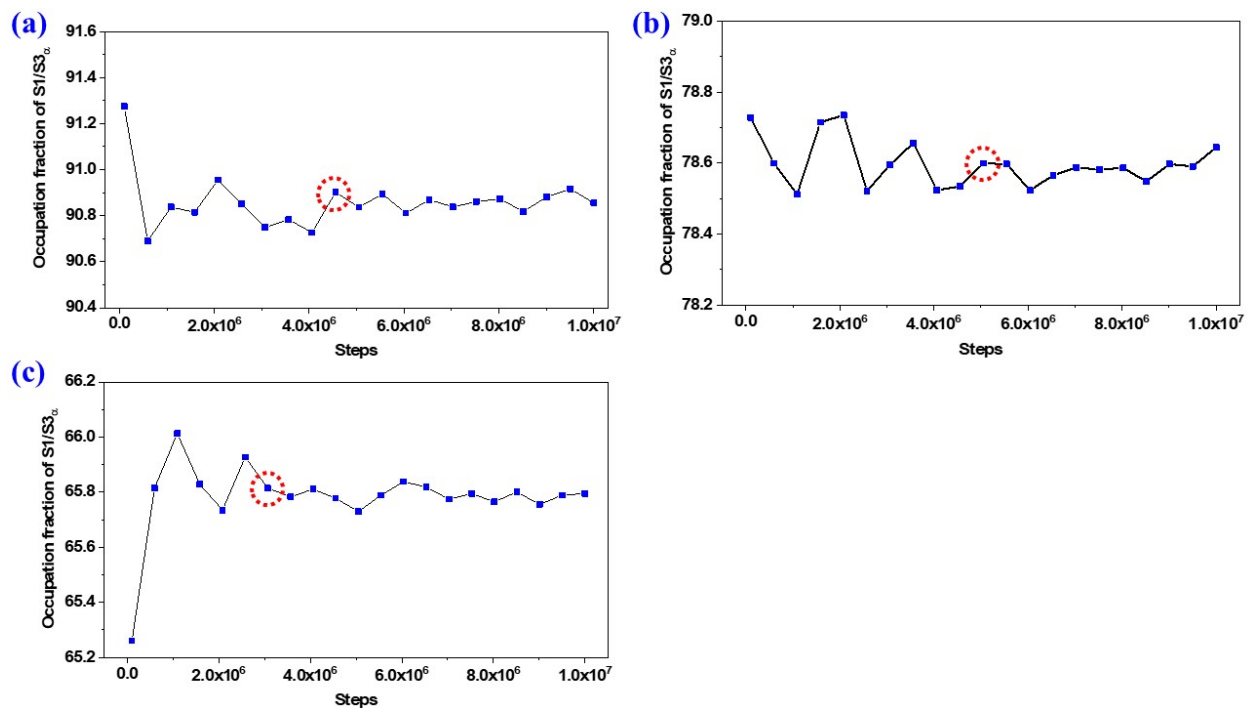
Figure S3 Equilibration plots for the kinetic Monte Carlo simulation of PtCO@LTA at 300 (a), 500 (b) and 800 K (c).

4. Effect of confinement on $Pt_5(CO)_m$ cluster structures
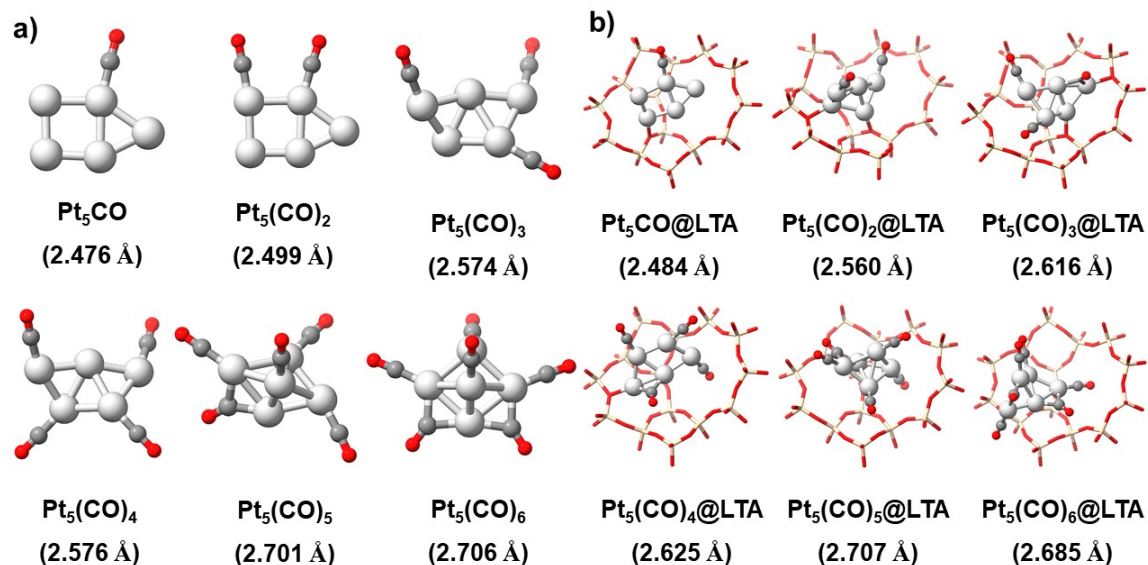
Figure S4 Putative global minimum $Pt_5(CO)_m$ configurations of a) vacuum phase and b) zeolite encapsulated clusters $Pt_5(CO)_m$ (m < 7). The average Pt-Pt bond lengths are given in parentheses.

Table S1 Average bond length and magnetization of vacuum phase global minimum $Pt_5(CO)_m$ clusters

$Pt_5(CO)_m$	$<r(Pt-Pt)>$ (Å)	$<r(Pt-C)>$ (Å)	$<r(C-O)>$ (Å)	Magnetization (μ_B)
1	2.476	1.826	1.165	2.00
2	2.499	1.826	1.164	2.00
3	2.574	1.824	1.165	2.00
4	2.576	1.826	1.164	0.00
5	2.701	1.884	1.167	0.00
6	2.706	1.929	1.168	0.00

Table S2 Average bond length and magnetization of zeolite encapsulated global minimum $Pt_5(CO)_m$ clusters

$Pt_5(CO)_m$	$<r(Pt-Pt)>$ (Å)	$<r(Pt-C)>$ (Å)	$<r(C-O)>$ (Å)	Magnetization (μ_B)
1	2.484	1.816	1.170	2.00
2	2.560	1.827	1.169	0.00
3	2.616	1.875	1.177	0.00
4	2.625	1.865	1.173	0.00
5	2.707	1.880	1.168	0.00
6	2.685	1.921	1.169	0.00

5. Dissociation energy of vacuum phase $Pt_4(CO)_m$
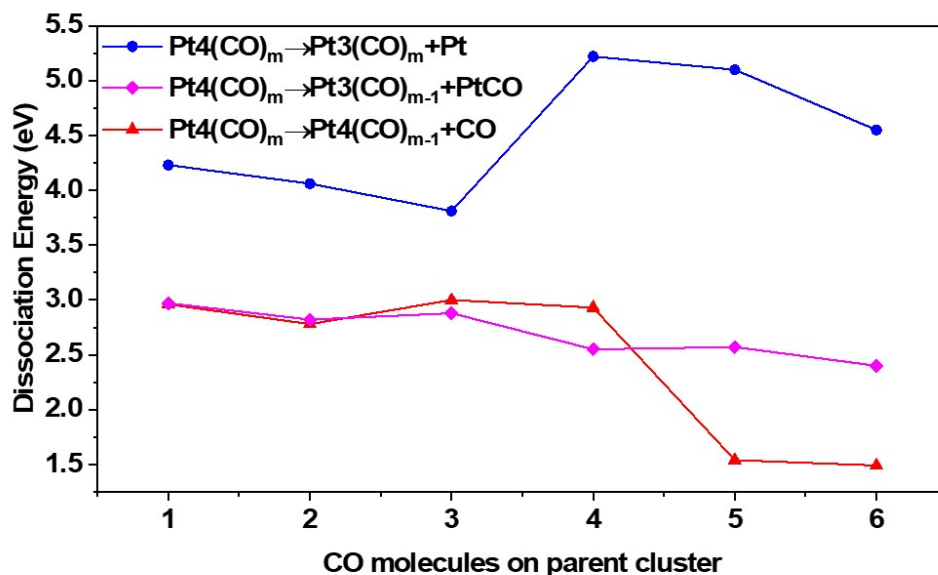
Figure S5 The dissociation of vacuum phase $Pt_4(CO)_m$ cluster with respect to CO, Pt and PtCO

Table S 3 The dissociation of vacuum phase $Pt_4(CO)_m$ cluster with respect to CO, Pt and PtCO

$Pt_4(CO)_m$	1	2	3	4	5	6
$E_{diss}(CO)$ (eV)	+2.96	+2.78	+3.00	+2.93	+1.54	+1.49
$E_{diss}(Pt)$ (eV)	+4.23	+4.06	+3.81	+5.22	+5.10	+4.55
$E_{diss}(PtCO)$ (eV)	+2.97	+2.82	+2.88	+2.55	+2.57	+2.40

*$E_{diss}(CO)$, $E_{diss}(Pt)$ and $E_{diss}(PtCO)$ represent the energy required to separate single CO, Pt and PtCO from the $Pt_4(CO)_m$ cluster and form the vacuum phase single CO, Pt and PtCO structure, respectively.

6.　Dissociation energy of zeolite encapsulated $Pt_4(CO)_m$

Figure S6 The dissociation of zeolite encapsulated $Pt_4(CO)_m$ cluster with respect to CO, Pt and PtCO

Table S4 The dissociation of zeolite encapsulated $Pt_4(CO)_m$ cluster with respect to CO, Pt and PtCO

$Pt_4(CO)_m$@LTA	1	2	3	4	5	6
$E_{diss}(CO)$ (eV)	+2.68	+2.63	+2.63	+2.39	+1.18	+1.41
$E_{diss}(Pt)$ (eV)	+2.14	+1.84	+2.08	+2.91	+2.94	+2.59
$E_{diss}(PtCO)$ (eV)	+1.74	+1.82	+1.52	+1.52	+1.14	+1.40

*$E_{diss}(CO)$, $E_{diss}(Pt)$ and $E_{diss}(PtCO)$ represent the energy required to separate single CO, Pt and PtCO from the zeolite encapsulated $Pt_4(CO)_m$ cluster and form the global minimum CO@LTA, Pt@LTA and PtCO@LTA structure, respectively.

7. Dissociation energy of vacuum phase $Pt_5(CO)_m$
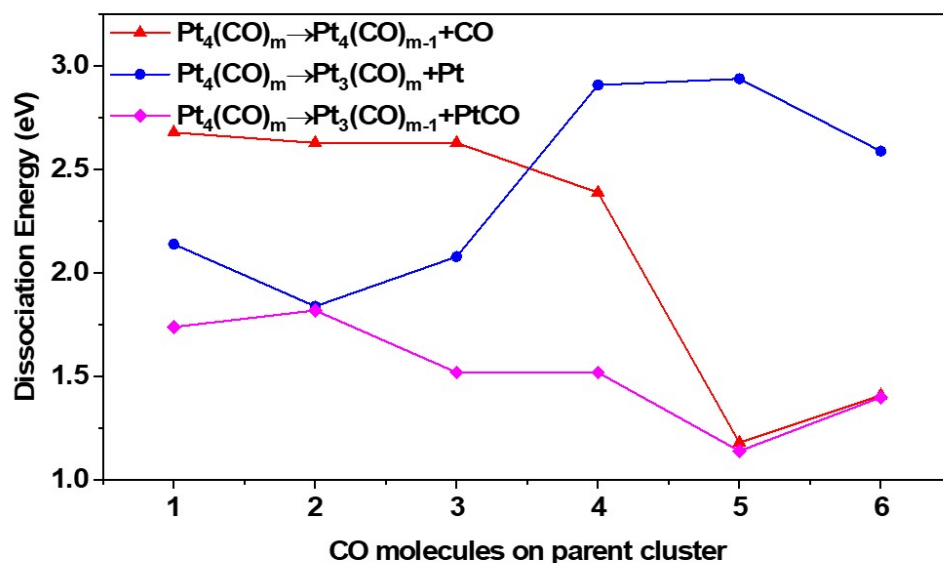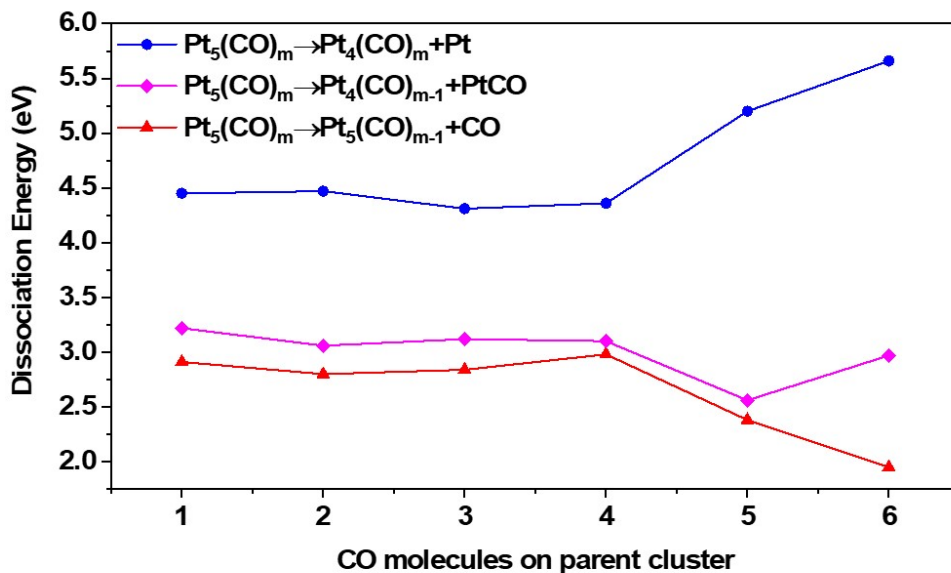

Figure S7 The dissociation of vacuum phase $Pt_5(CO)_m$ cluster with respect to CO, Pt and PtCO

Table S5 The dissociation of vacuum phase $Pt_5(CO)_m$ cluster with respect to CO, Pt and PtCO

$Pt_5(CO)_m$	1	2	3	4	5	6
$E_{diss}(CO)$ (eV)	+2.91	+2.80	+2.84	+2.98	+2.38	+1.95
$E_{diss}(Pt)$ (eV)	+4.45	+4.47	+4.31	+4.36	+5.20	+5.66
$E_{diss}(PtCO)$ (eV)	+3.22	+3.06	+3.12	+3.10	+2.56	+2.97

*$E_{diss}(CO)$, $E_{diss}(Pt)$ and $E_{diss}(PtCO)$ represent the energy required to separate single CO, Pt and PtCO from the $Pt_5(CO)_m$ cluster and form the vacuum phase single CO, Pt and PtCO structure, respectively.

# 8. Dissociation energy of zeolite encapsulated Pt$_5$(CO)$_m$
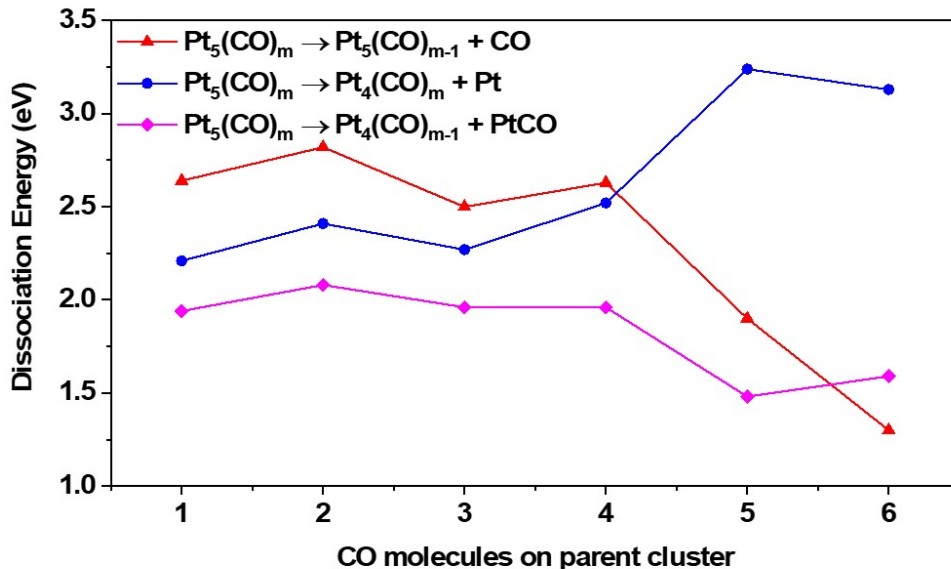
Figure S8 The dissociation of zeolite encapsulated Pt$_5$(CO)$_m$ cluster with respect to CO, Pt and PtCO

Table S6 The dissociation of zeolite encapsulated Pt$_5$(CO)$_m$ cluster with respect to CO, Pt and PtCO

Pt$_5$(CO)$_m$@LTA	1	2	3	4	5	6
E$_{diss}$(CO) (eV)	+2.64	+2.82	+2.50	+2.63	+1.90	+1.30
E$_{diss}$(Pt) (eV)	+2.21	+2.41	+2.27	+2.52	+3.24	+3.13
E$_{diss}$(PtCO) (eV)	+1.94	+2.08	+1.96	+1.96	+1.48	+1.59

*E$_{diss}$(CO), E$_{diss}$(Pt) and E$_{diss}$(PtCO) represent the energy required to separate single CO, Pt and PtCO from the zeolite encapsulated Pt$_5$(CO)$_m$ cluster and form the global minimum CO@LTA, Pt@LTA and PtCO@LTA structure, respectively.

9. Adsorption energy of vacuum phase and zeolite encapsulated $Pt_5(CO)_m$ cluster
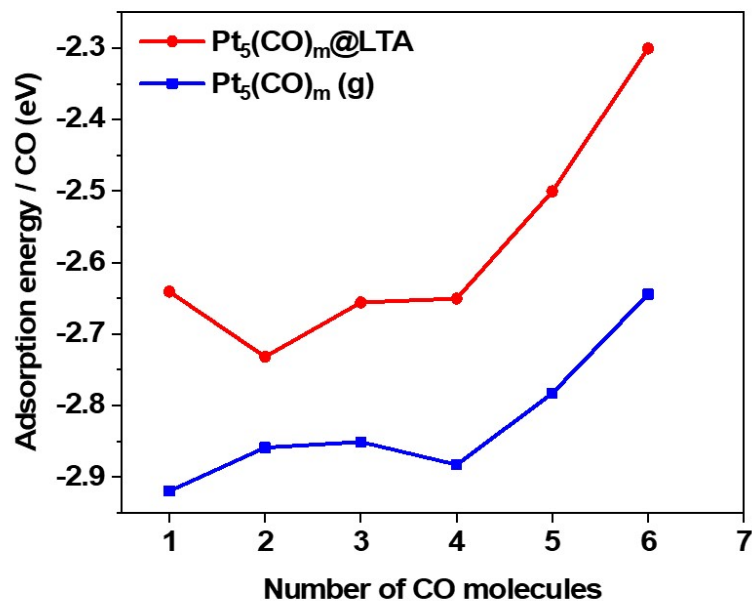
Figure S9 The adsorption energy per CO molecule on global minimum vacuum phase and zeolite encapsulated $Pt_5(CO)_m$ clusters. The role of confinement inside the pore of the metal cluster upon the binding of CO molecules is demonstrated by the significant reduction in the per CO molecule adsorption energies.

10. Energetic data for $Pt_1(CO)_m@LTA$

The role of CO loading on the stability of Pt in LTA was considered, by binding of multiple CO molecules to Pt@LTA and Pt(g). For both isolated and zeolite-encapsulated Pt, the limiting number of CO molecules (m) which associate with Pt is four. The complexes in the zeolite are structurally similar to those *in vacuo* (Figure S4). $Pt(CO)_2$ is a bent linear complex, $Pt(CO)_3$ is a trigonal planar structure and $Pt(CO)_4$ adopts a tetrahedral configuration. The adsorption energy of CO is substantially reduced in the encapsulated complexes with respect to the *vacuo* complexes (Table S1). Furthermore, the adsorption energy per CO decreases monotonically with increasing m for both vacuum and encapsulated $Pt(CO)_m$ complexes. The weakening Pt-CO bonds are reflected in the increasing average Pt-C and decreasing average C-O bond lengths as the loading of CO molecules increases.

Table S7 Energetic data for $Pt(CO)_m$ complexes. Values in parentheses are for corresponding vacuum complexes

n	E_{ads} (eV) / CO	E_{inc} (eV)	$q(Pt)$ (e^-)	$<r(Pt-C)>$ (Å)	$<r(C-O)>$ (Å)	$Pt-O_f$ (Å)
1	-2.95 (-3.84)	-1.38	+0.05 (+0.03)	1.780 (1.757)	1.169 (1.167)	2.160
2	-2.18 (-3.12)	-0.63	+0.16 (+0.16)	1.878 (1.833)	1.159 (1.157)	3.672
3	-1.80 (-2.46)	-0.74	+0.32 (+0.29)	1.922 (1.924)	1.158 (1.158)	3.920
4	-1.51 (-2.04)	-0.84	+0.34 (+0.33)	1.954 (1.954)	1.156 (1.156)	4.139

The most significant effect of CO loading on encapsulated Pt is to detach the Pt atom from the framework. For m>1, the $Pt(CO)_m$ complex becomes volatile, occupying the free space in the α-cage, with no covalent bonds to the framework. The powerful effect of CO in dispersing Pt clusters into smaller units is well-established in the literature, both on oxide surfaces and in zeolites.[1-5] The global minimum configurations for all volatile complexes are found to involve one CO molecule occupying the centre of the eight-ring. This is a dispersion-driven effect, with no formation of covalent bonds or strain of the eight-ring.

The incorporation energies of the $Pt(CO)_m$ complexes show the preference for incorporation of the entire complex into the zeolite. E_{inc} is therefore a combination of energetic contributions, including binding energy to the framework, dispersive stabilisation in the pore, and steric strain due to

confinement in the alpha cage. The total incorporation energy decreases in magnitude from PtCO to $Pt(CO)_2$, which is consistent with the loss of the Pt-O framework bond. E_{inc} then increases in magnitude from $Pt(CO)_2$ to $Pt(CO)_4$, as additional CO molecules stabilise the volatile complex in the pore. For all CO loadings, E_{inc} is negative, which implies that overall, the loss of framework binding is overcome by the gain in favourable dispersive interactions between $Pt(CO)_m$ and the zeolite framework.
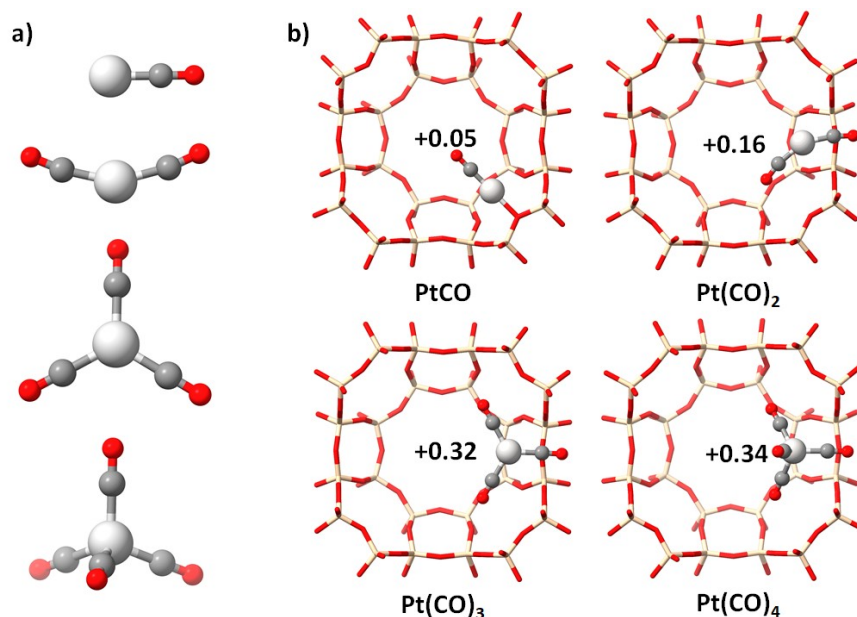
Figure S10 Structures of global minimum $Pt(CO)_m$ complexes (m<5) in a)vacuo, b)LTA (Pt Bader charge is labelled).

Ab initio dynamics simulations were performed for $Pt(CO)_m$, in order to determine whether any atom trapping was present, despite the lack of framework-association on the potential energy surface. 10 ps equilibration simulations were run at 450 K. In all cases, except PtCO, which is bound to the framework, the complexes moved freely inside the α-cage, and did not transfer between cages on the timescale of the simulation. No bond formation between complex and framework was observed. For m = 1, 2 and 3, the complex was stable, while $Pt(CO)_4$ exhibited transient dissociation and re-association of one CO molecule, which is consist with the findings that $Pt(CO)_4$ and $Pd(CO)_4$ are not stable at room temperature.[6, 7]

11. Ab initio Molecular Dynamics of Pt(CO)$_m$@LTA
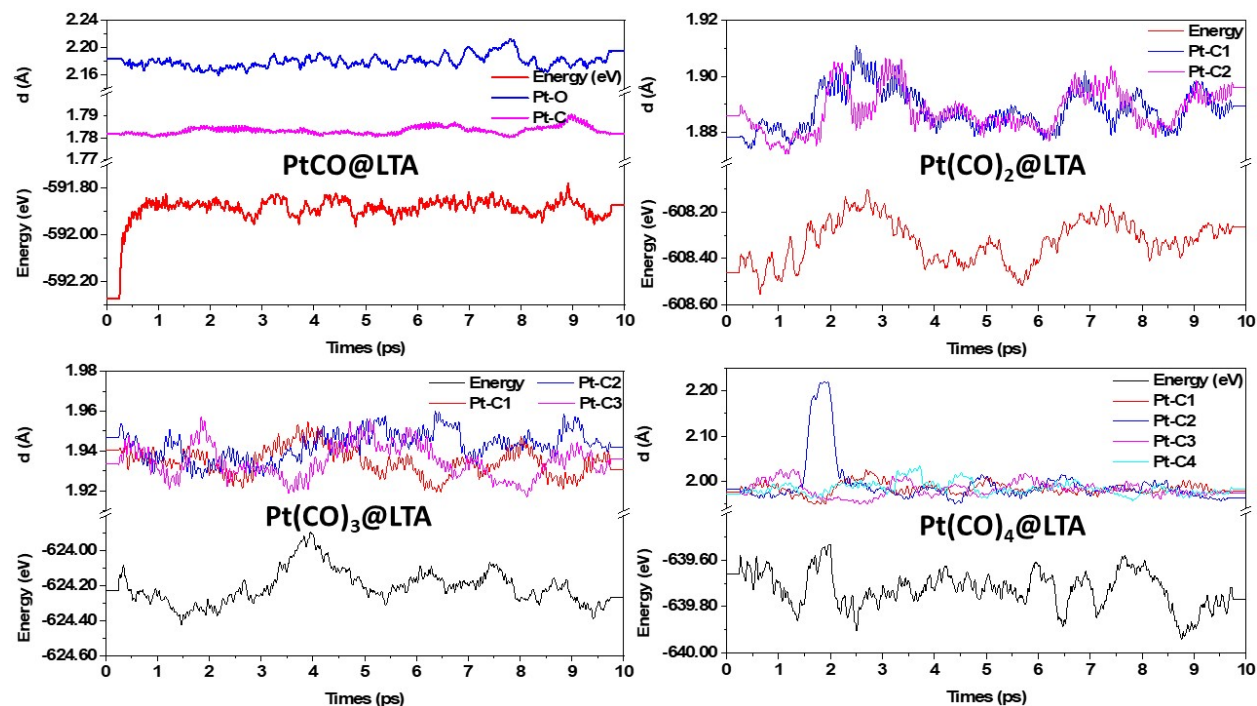
Figure S11 Trace of the total internal energy running average and Pt-C bond length running average of a 10 ps Ab initio Molecular Dynamics simulation of Pt(CO)$_m$@LTA at 450 K in the NVT thermodynamic ensemble. A range of 0.5 ps (1000 MD steps) was used to calculate running averages. Pt-C bond lengths increase monotonically as the number of bound CO molecules increases. Structures obtained with DFT have average Pt-C bond lengths of 1.780, 1.878, 1.922 and 1.954 Å for Pt(CO)$_m$@LTA (m=1-4), respectively. CO binding is stable over the timescale of the simulation, with the exception of Pt(CO)$_4$, for which spontaneous detachment of a CO molecule occurs at around 1.5 ps, followed by reattachment at around 2 ps.

12. Kinetic Monte Carlo simulation of PtH$_2$@LTA
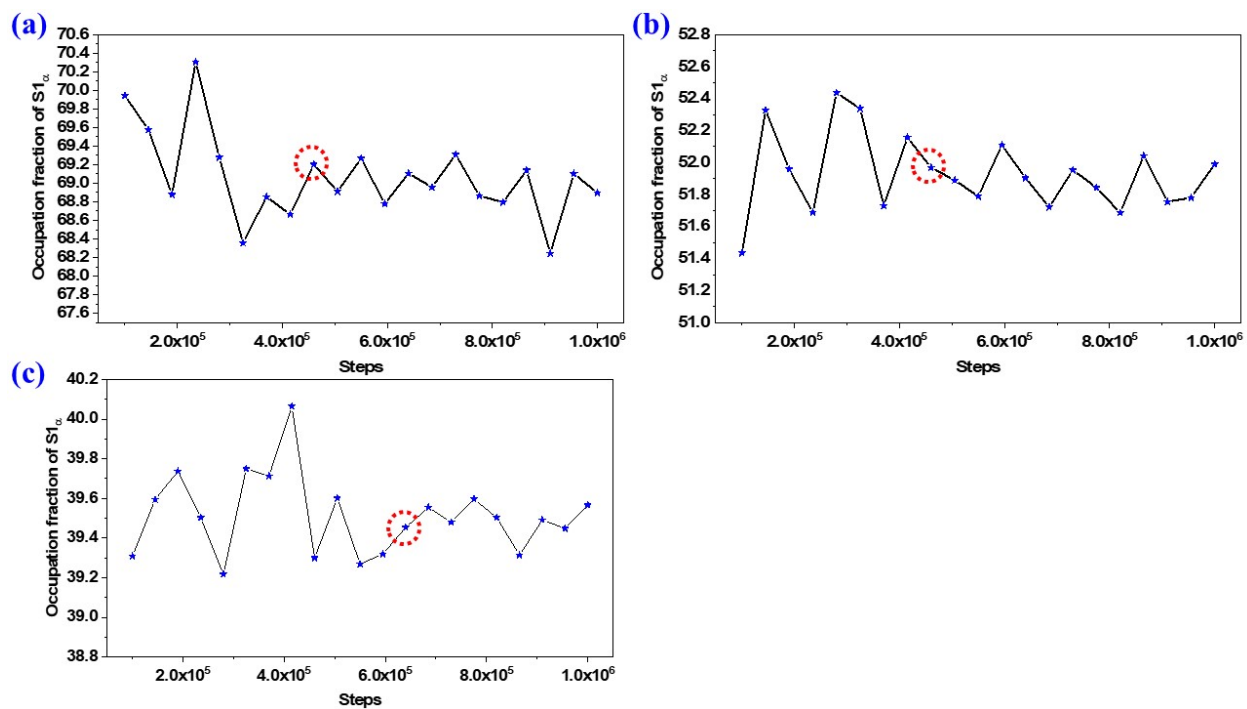
Figure S12 Equilibration plots for the kinetic Monte Carlo simulation of PtH$_2$@LTA at 300 (a), 500 (b) and 800 K (c).

13. Au-X@LTA (X=CO, H$_2$)

The effect of adsorbates on the energetics and structures of Au@zeolite configurations was probed using CO and H$_2$ molecules. We find that the Au(CO)$_m$ complexes exhibit somewhat different geometries to the Pt(CO)$_m$ complexes. For m=1, the PtCO complex remains attached to the framework, while AuCO shows no framework attachment, and adopted a bent structure. This has previously been observed in calculations of *vacuo* AuCO complexes.[8, 9] For m=2, Pt(CO)$_2$ has a bent-linear geometry, while Au is linear. For m=3, the structures are similar. However, for all cases, the binding energies to Au are significantly lower than to Pt. AuCO, Au(CO)$_2$ and Au(CO)$_3$ all adopt configurations in which the CO molecule occupies the eight-ring, and no strong interactions are formed between the metal site and the framework (Figure S11). Unlike in the case of Pt(CO)$_m$, the binding energy of CO is not significantly reduced upon confinement within the pore (Table S8). No local minimum was obtained for the Au(CO)$_4$ complex, which implies that the Au atom has a smaller capacity for CO binding than Pt.

Table S8 Energetic data for Au(CO)$_m$ complexes. Values in parentheses are for corresponding vacuum complexes

n	E$_{ads}$ (eV) / CO	E$_{inc}$ (eV)	q(Pt) (e$^-$)	<r(Au-C)> (Å)	<r(C-O)> (Å)
1	-0.90 (-0.84)	-0.69	+0.02 (-0.05)	1.969 (1.970)	1.160 (1.162)
2	-1.01 (-1.17)	-0.55	+0.29 (+0.29)	1.919 (1.919)	1.166 (1.166)
3	-0.80 (-0.92)	-0.72	+0.33 (+0.32)	1.973 (1.973)	1.160 (1.160)

Au forms weak complexes with H$_2$, with long Au-H bond lengths of greater than 2 Å (c.f. 1.53 Å for PtH$_2$). The H-H bonds are increased negligibly, from 0.750 Å to 0.777, 0.778 and 0.779 Å in S2, S1 and S3, respectively. Overall, Au is a poor attractor of reducing adsorbates, and is largely unperturbed by the presence of the zeolite framework, in contrast to Pt.
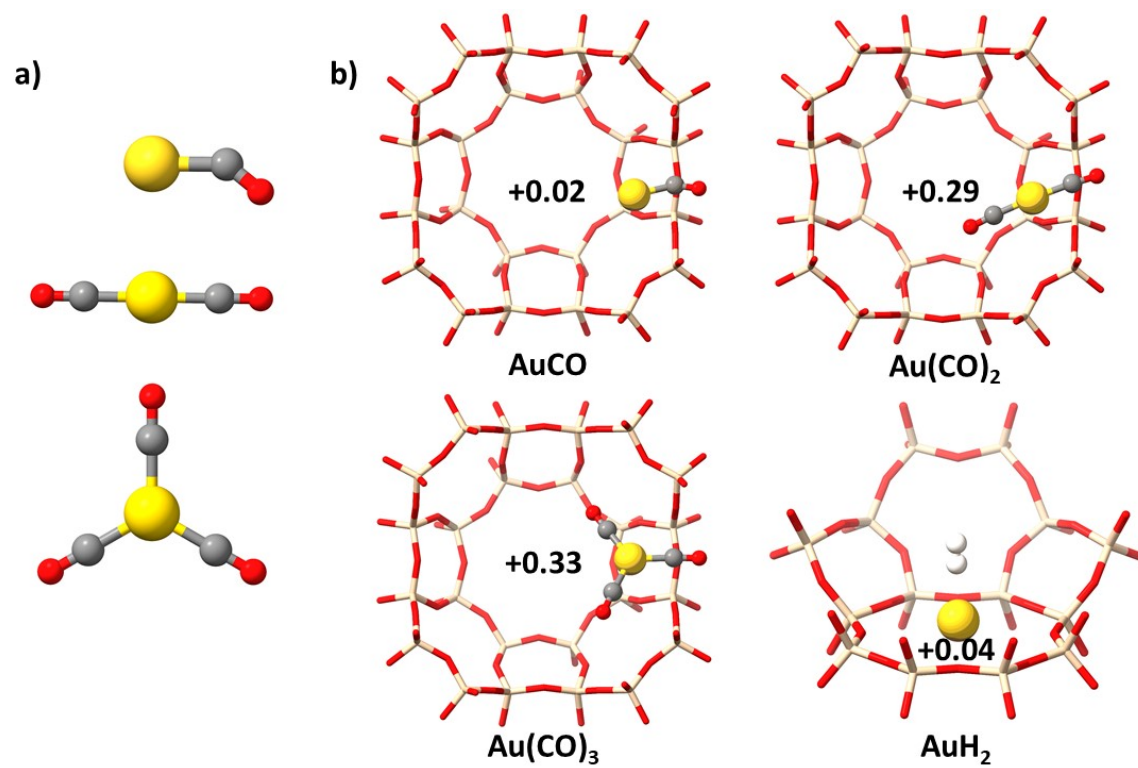
Figure S13 Structures of global minima for Au(CO)$_m$ (m<4) in a)vacuo, b)LTA, in addition to the global minimum for AuH$_2$@LTA (bottom right).

References

1.   Y. Akdogan, S. Anantharaman, X. Liu, G. K. Lahiri, H. Bertagnolli and E. Roduner, *J. Phys. Chem. C*, 2009, **113**, 2352-2359.

2.   N. Chaâbane, R. Lazzari, J. Jupille, G. Renaud and E. Avellar Soares, *J. Phys. Chem. C*, 2012, **116**, 23362-23370.

3.   M. Keppeler, G. Bräuning, S. G. Radhakrishnan, X. Liu, C. Jensen and E. Roduner, *Catal. Sci. Technol.*, 2016, **6**, 6814-6823.

4.   B. L. Mojet and D. C. Koningsberger, *Catal. Lett.*, 1996, **39**, 191-196.

5.   R. Bliem, J. E. S. van der Hoeven, J. Hulva, J. Pavelec, O. Gamba, P. E. de Jongh, M. Schmid, P. Blaha, U. Diebold and G. S. Parkinson, *Proc. Natl. Acad. Sci. U.S.A.*, 2016, **113**, 8921.

6.   E. P. Kuendig, D. McIntosh, M. Moskovits and G. A. Ozin, *J. Am. Chem. Soc.*, 1973, **95**, 7234-7241.

7.   M. Doerr and G. Frenking, *Z. Anorg. Allg. Chem.*, 2002, **628**, 843-850.

8.   B. Liang and L. Andrews, *J. Phys. Chem. A*, 2000, **104**, 9156-9164.

9.   N. S. Phala, G. Klatt and E. v. Steen, *Chem. Phys. Lett.*, 2004, **395**, 33-37.